Journal of Colloid and Interface Science 323 (2008) 235–241

Contents lists available at ScienceDirect

Journal of Colloid and Interface Science

www.elsevier.com/locate/jcis

Modeling of vapor sorption in polymeric film studied by surface plasmon resonance spectroscopy

M. Erdoğan [a,*], İ. Çapan [a], Ç. Tarimci [b], A.K. Hassan [c]

[a] Balıkesir University, Faculty of Art and Sciences, Department of Physics, Cagis Campus, 10145 Balikesir, Turkey
[b] Ankara University, Faculty of Engineering, Department of Engineering Physics, 06100 Ankara, Turkey
[c] Materials and Engineering Research Institute, Sheffield Hallam University, Sheaf Building, Pond Street, Sheffield S1 1WB, UK

ARTICLE INFO

Article history:
Received 28 January 2008
Accepted 21 April 2008
Available online 25 April 2008

Keywords:
Vapor sorption
Chemical sensor
Poly(methyl methacrylate) film
Diffusion

ABSTRACT

Sorption process by surface plasmon resonance (SPR) was studied by exposing polymeric film made from anthracene labeled poly(methyl methacrylate) (An-PMMA) chains to various concentrations of saturated chloroform vapor. It was observed that the reflectivity changes were fast and reversible. The changes in reflectivity implied the swelling behavior of polymeric film during adsorbtion and can be explained by capturing of chloroform molecules. When clean air is introduced into gas cell similar behavior is observed but this time in the opposite direction as a result of desorption. Fick's law for diffusion was used to quantify real time SPR data for the swelling and desorption processes. It was observed that diffusion coefficients (D_s) for swelling obeyed the $t^{1/2}$ law and found to be correlated with the amount of chloroform content in the cell. Diffusion coefficients (D_d) during desorption were also measured and found to be increased as the saturated chloroform vapor content is increased in the cell.

Published by Elsevier Inc.

1. Introduction

Polymeric materials are often used as environmentally responsive coatings in sensors due to their ability to absorb a variety of different molecules. The versatility of polymers makes them usable in many sensor types based on different transduction principles for the detection of a variety of analytes. Polymer chains are flexible, and molecules can easily be absorbed into polymer networks. This absorbtion process results in a swelling and a mass increase of the polymer materials.

Moisture and organic vapor sorption in polymeric films and their concurrent swelling is important in many applications, such as coating, microelectronics manufacturing and chemical sensors. Conventional gravimetric methods are not always suitable for studying these phenomena in polymeric films [1]. Although there is extensive literature on polymer swelling, only in recent years extensive work has been performed to exploit this phenomenon for chemical sensing. The lifetime of most sensors based on polymer swelling is limited by delamination of the polymeric film [2].

The major difficulty in gas identification is the fabrication of stable sensors with high sensitivity and very good selectivity of the substance to be detected. Several measurement techniques such as Surface Plasmon Resonance (SPR) and Quartz Crystal Microbalance (QCM) are used to monitor and detect various chemical gases because of their wide range of potential applications. An example is environmental monitoring, such as detecting the presence and concentration of toxic or otherwise dangerous gases that are released through spillage or leakage [3]. Another broad application area is quality control and industrial monitoring, particularly in such industries as food processing, perfume, beverage and other chemical products [4,5]. Monitoring and determining the constituents of a sample gas typically involves collecting samples and analyzing them in a gas chromatograph–mass spectrometer (GC–MS) of significant size and cost [6]. Although GC–MS systems work very well, many applications need sensor systems that are smaller, more portable, cheaper and even disposable [7].

SPR is a total internal reflection system with a thin metal film on top of the high-index dielectric surface. The resonance of surface polaritons at the metal-dielectric interface is extremely sensitive to the dielectric constant and thickness of the medium adjacent to the metal film [8–10]. Using flow-injection type electrochemical SPR sensing system, adsorption and desorption of water-soluble polymers on gold surfaces have been observed [11]. It has also been found that lightly crosslinked molecularly imprinted polymer particles can serve as the basis of a sensitive and selective membrane for the detection of organic contaminants such as pharmaceuticals in aquatic environments [12].

In the present work polymeric film formed from anthracene labeled linear poly(methyl methacrylate) (An-PMMA), chains were subjected to various concentrations of partially saturated chloroform vapors to study swelling and desorption mechanism. Using SPR measurement system, variations in the intensity of reflected

* Corresponding author. Fax: +90 266 612 12 15.
E-mail address: merdogan@balikesir.edu.tr (M. Erdoğan).

0021-9797/$ – see front matter Published by Elsevier Inc.
doi:10.1016/j.jcis.2008.04.045

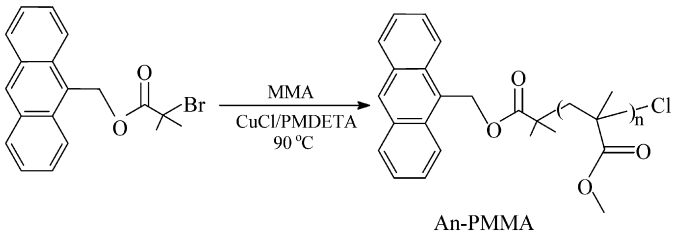

Scheme 1. Synthesis of poly(methyl methacrylate).

light was monitored in real time during swelling in which organic vapor is introduced into a gas cell and desorption when clean air is injected into it. The organic vapor uptake causes an increase in the transparency of polymeric film that explains the changes in reflected light intensity during swelling and desorption. Fick's second law for diffusion [13] was employed to determine the diffusion coefficients for the swelling and desorption processes.

2. Materials and methods

2.1. Synthesis of poly(methyl methacrylate)

The general procedure for atom transfer radical polymerization (ATRP) was followed; to a Schlenk tube equipped with magnetic stirring bar, ligand, catalyst, degassed monomer, solvent and initiator were added in the mentioned order. Tube was degassed by freeze–pump–thaw cycles, left under vacuum and placed in thermostated oil bath at a constant temperature of 90 °C. After polymerization, the reaction mixture was diluted with tetrahydrofuran (THF) and then passed through a column of neutral alumina to remove metal salt. The excess of THF and unreacted monomer were evaporated under reduced pressure. PMMA samples were dissolved in THF and precipitated in methanol, filtered and dried overnight in vacuum oven at 50 °C. This procedure was repeated at least twice for the sample in order to remove unbounded initiator species if there are any. The conversions were determined gravimetrically. PMMA was prepared in 50 vol% diphenylether (DPE) solution at 90 °C using CuCl/*N*,*N*,*N*′,*N*″,*N*″-pentamethyldiethylenetriamine (PMDETA) as the catalyst and 9-anthryl methyl 2-bromo-2-methyl propanoate, as the initiator. This led to the formation of anthracene labeled poly(methyl methacrylate)s (An-PMMA)s. Syntheses of poly(methyl methacrylate) were prepared as illustrated in Scheme 1. Details and characterization of polymer chains are given in the literature [14].

2.2. Deposition of polymeric films

For the SPR measurements 50 nm thick gold layer was thermally evaporated onto the glass substrates with the rate of 2 nm s^{-1} under vacuum of about 10^{-3} Pa. Solution of An-PMMA molecules was prepared using chloroform as a solvent at a concentration of 2 mg ml^{-1}. Spin coating of the An-PMMA polymer was performed by dispensing 100 μl of solution onto the gold coated substrate which was rotating with a rotation speed of 2000 rpm. For the spectroscopic ellipsometry measurements thin films were fabricated onto silicon substrates using the same film fabrication procedure. Woolam M-2000VTM model spectroscopic ellipsometry rotating analyzer in the spectral range of 370–1000 nm was used where the angle of incidence have been fixed at 70°.

2.3. Characterization of polymeric films

Spectroscopic ellipsometry which is based on measuring and analyzing the polarization change of the reflected light was employed for the characterization of the An-PMMA polymer films. In this technique, the measured ellipsometric parameters $\psi(\lambda)$ and $\Delta(\lambda)$ which are the angles related to the polarization change of the light caused by its interaction with a sample are used to obtain thickness, refractive index and extinction coefficients of the polymer films [15]. The relation of the ellipsometric parameters with the p and s components of the polarized incident wave can be expressed by $R_p/R_s = \tan(\psi)\exp(i\Delta)$ where $\tan(\psi)$ is the ratio of amplitudes and Δ is the phase difference between p and s components of polarized light. The optical parameters were obtained using software based on Fresnel reflection equations.

2.4. SPR set-up and gas sensing measurements

The experimental SPR set-up was based on the Kretschmann configuration [16] and was identical to that reported elsewhere [17]. The thin film coated slides and semi-cylindrical prism (with a refractive index of 1.515) were brought into optical contact using ethyl salicylate (99% Aldrich) as an index matching fluid. P-polarized beam with a wavelength of 632.8 nm was obtained using a He–Ne laser source for the excitation of surface plasmons. The prism and sample combination were placed on a θ–2θ rotation stage driven by a microprocessor controlled stepping motor (with resolution of 0.01°) to record SPR curves which shows the variation of the reflected light intensity against the angle of incidence. For the kinetic measurement, poly (tetrafluoro ethylene) (PTFE) gas cell with a rubber O-ring was sealed by the coated slides to allow measurements of the reflected light intensity as a function of time at a fixed angle θ^* during vapor exposures. Different concentrations of saturated chloroform vapor were mixed with dry air in a sealed syringe and injected into the gas cell for 2 min followed by 2 min recovery by injecting dry air into the gas cell.

2.5. Theoretical consideration

When Fick's second law of diffusion is applied to a plane sheet and solved by assuming a constant diffusion coefficient, the following equation is obtained for concentration changes in time [13]:

$$\frac{C}{C_0} = \frac{x}{a_0} + \frac{2}{\pi}\sum_{n=1}^{\infty}\frac{\cos n\pi}{n}\sin\frac{n\pi x}{a_0}\exp\left(-\frac{Dn^2\pi^2}{a_0^2}t\right), \tag{1}$$

where a_0 is the thickness of the slab, D is the diffusion coefficient, and C_0 and C are the concentration of the diffusant at time zero and t, respectively. x corresponds to the distance at which C is measured. We can replace the concentration terms directly with the amount of diffusant by using

$$M = \int_V C\,dV. \tag{2}$$

When Eq. (2) is considered for a plane volume element and substituted in Eq. (1), the following solution is obtained [13].

$$\frac{M_t}{M_\infty} = 1 - \frac{8}{\pi^2}\sum_{n=0}^{\infty}\frac{1}{(2n+1)^2}\exp\left(-\frac{(2n+1)^2D\pi^2}{a_0^2}t\right), \tag{3}$$

where M_t and M_∞ represent the amount of diffusant entering the plane sheet at time t and infinity, respectively. This equation can be reduced to a simplified form still 99% accurate:

$$\frac{M_t}{M_\infty} = 4\sqrt{\frac{D}{\pi a_0^2}t^{1/2}}, \tag{4}$$

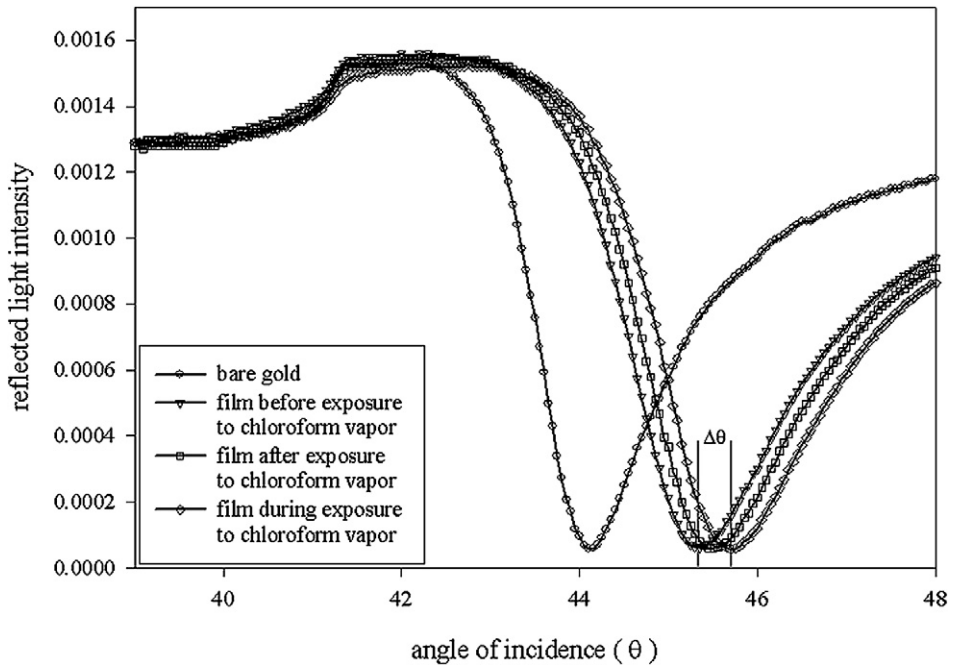

Fig. 1. SPR curves showing the variation of reflected light intensity as a function of angle of incidence θ for bare gold and An-PMMA polymeric film during and after exposure to saturated chloroform vapor.

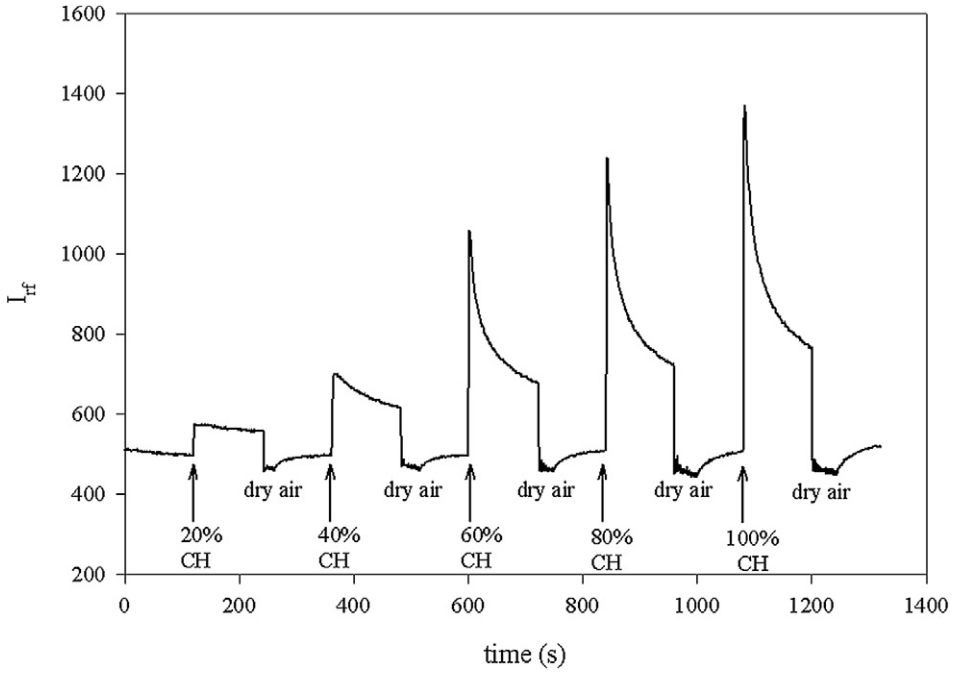

Fig. 2. The variation of intensity of reflected light as a function of time when the An-PMMA polymeric film is exposed to various concentrations of saturated chloroform vapor.

which is called early-time equation and this square root relation can be used to interpret for the swelling data. As the term $n = 0$ is taken and the other terms are omitted from the series expansion in Eq. (3), Crank also derived the following equation.

$$\frac{M_t}{M_\infty} = 1 - \frac{8}{\pi^2}\exp\left[\frac{\pi^2 D}{a_0^2}t\right]. \tag{5}$$

This equation is termed late-time equation and mainly used to obtain desorption diffusion coefficients, D_d during the release of the diffusant from swollen materials such as polymeric films, gels, etc.

3. Results and discussion

Fig. 1 shows a set of experimental SPR curves showing the variation of reflected light intensity as a function of angle of incidence θ. The gold coated glass substrate gives a minima of the SPR curve at 44.09°. This minimum was shifted to 45.32° after this substrate was coated with An-PMMA thin film layer. The SPR curve shift, $\Delta\theta$, due to injection of chloroform vapor into the gas cell was observed as 0.39° and is given by the following expression:

$$\Delta\theta = \frac{(2\pi/\lambda)(|\varepsilon_m|\varepsilon_i)^{3/2}d}{n_p \operatorname{Cos}\theta(|\varepsilon_m| - \varepsilon_i)^2\varepsilon}(\varepsilon - \varepsilon_i), \tag{6}$$

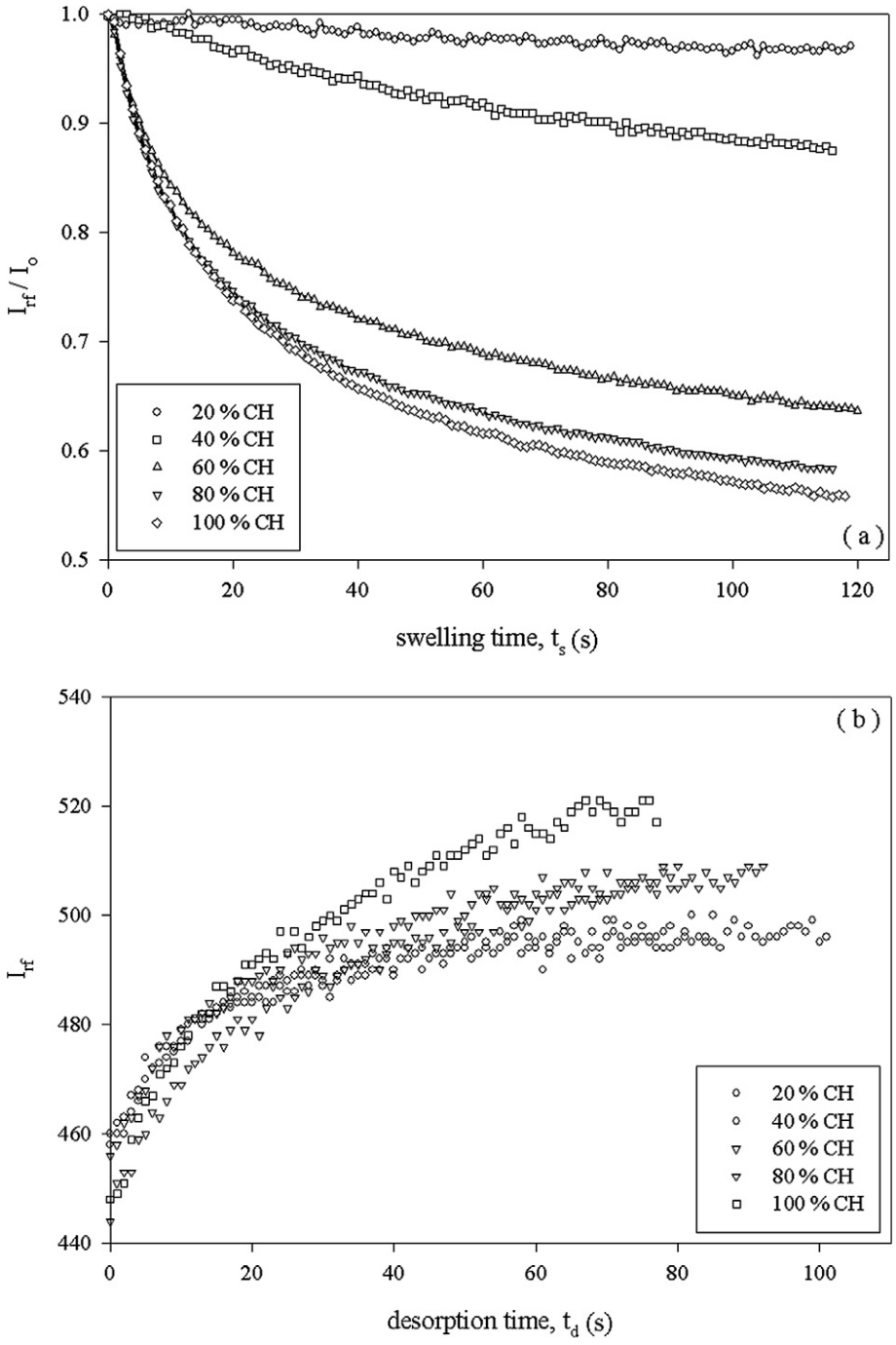

Fig. 3. Plot of reflected light intensity against swelling time, t_s (a) and desorption time, t_d (b).

where λ is the wavelength of the He–Ne laser light, n_p is the refractive index of the semi-cylindrical prism, $|\varepsilon_m|$ is the modulus of the complex dielectric constant of the gold film and ε_i is the dielectric medium in contact with the spun An-PMMA thin film layer. Using this equation the thickness of An-PMMA thin film was calculated without exposure, during exposure and after exposure to saturated chloroform vapor. The thickness values of An-PMMA film were found to be 8.69, 10.25 and 9.62 nm, respectively, by introducing the refractive index of the An-PMMA thin films as 1.4887 [18,19].

Using the spectroscopic ellipsometry fitting result for the same thin film onto silicon substrate, the thickness is found to be 8.14 ± 1.89 nm. This is in good agreement with the thickness value obtained from the theoretical fitting of the measured SPR curves.

Fig. 2 displays the kinetic measurement where reflected light intensity has been plotted as a function of time when the An-PMMA polymeric film was exposed to different contents of saturated chloroform vapor in air for 2 min followed by injection of clean air for another 2 min. The response against chloroform vapor is very fast, reversible and reproducible. The response is sharply increased for the first few seconds after injection of chloroform vapor and then tends to decrease exponentially. An-PMMA polymeric film shows a long term reproducible response to chloroform vapor.

In order to quantify the data given in Fig. 2, one has to extract the polymer film parameters due to swelling and desorption. Fig. 3 represents the normalized intensity of reflected light against swelling time (a) and desorption time (b) where the con-

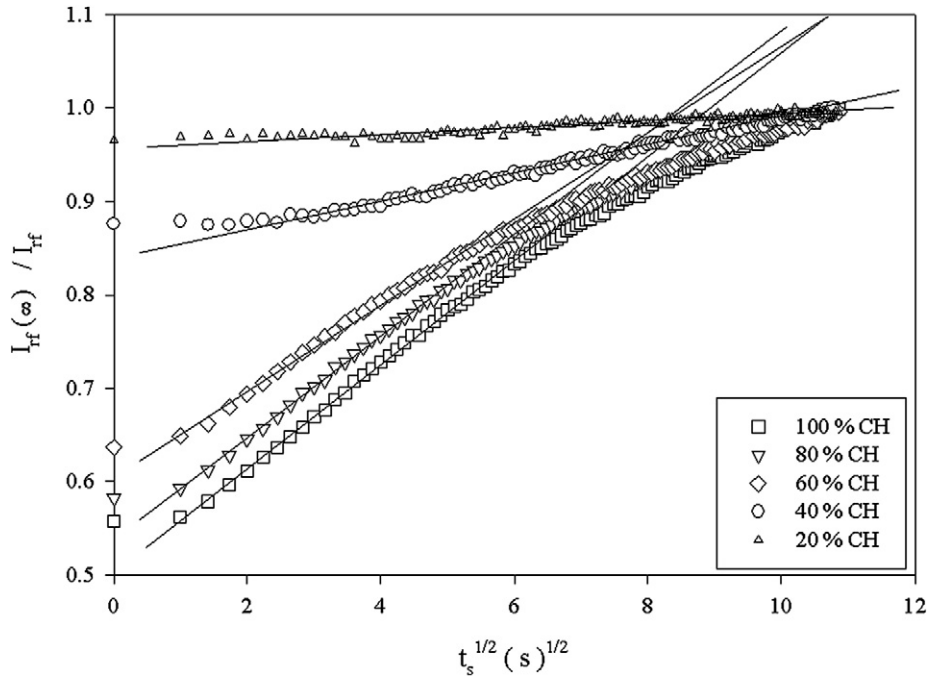

Fig. 4. Plot of reflected light intensity versus the square root of swelling time, $t_s^{1/2}$. Solid lines represent the fit of the data to Eq. (5).

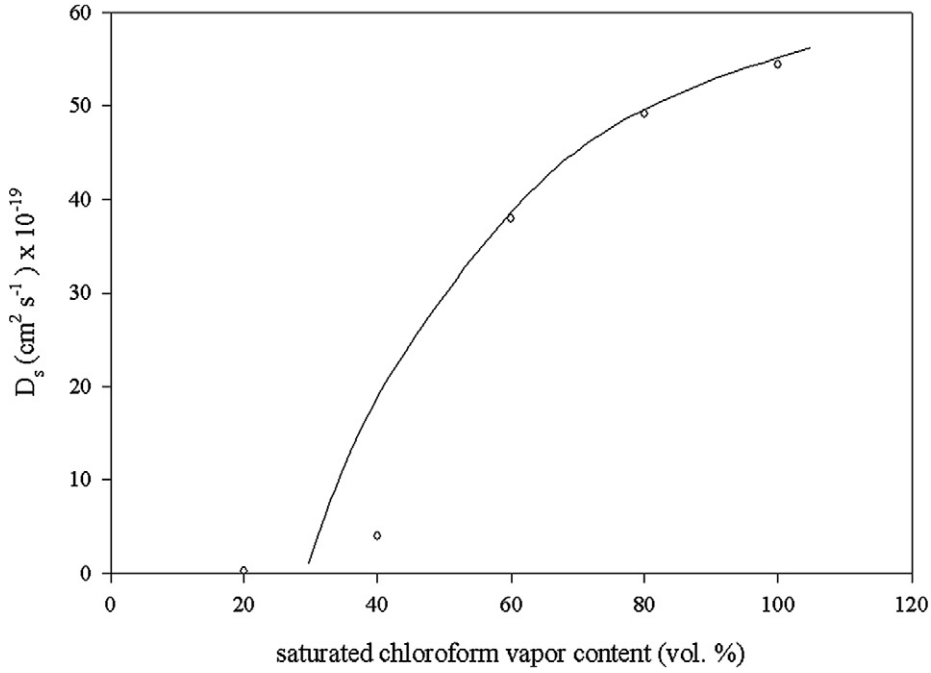

Fig. 5. The dependence of the swelling diffusion coefficients, D_s versus saturated chloroform vapor content.

solidation process involves setting starting times to $t = 0$ for each swelling and desorption cycles. As seen in Fig. 3a, the reflected light intensity, I_{rf} decreased as the time of vapor exposure is increased. It is also seen that changes in I_{rf} against the time of vapor exposure decreased very fast as the chloroform percentage concentration injected into the gas cell is increased. These behaviors can be explained with the chain interdiffusion between polymer chains during vapor exposure. As the saturated chloroform vapors penetrate into polymeric film, the polymer chains interdiffuse and transparency of the polymeric film increases, which results in the decrease of intensity of light reflected from the polymeric film. These results can be related to the amounts of diffusant entering the polymeric film M_t; that is, I_{rf} should be inversely proportional to M_t [20]. Equation (4) now can be written as

$$\left(\frac{I_{rf}(t)}{I_{rf}(\infty)}\right)^{-1} = 4\sqrt{\frac{D}{\pi a_0^2}}t^{1/2}, \tag{7}$$

where $I_{rf}(t)$ and $I_{rf}(\infty)$ are intensities of reflected light at any time, t and saturation point in I_{rf}, respectively. The normalized I_{rf} intensities $[I_{rf}(\infty)/I_{rf}(t)]$ are plotted in Fig. 4 for the square root of swelling time according to Eq. (7). The slopes of the linear relations in Fig. 4 produce the diffusion coefficients, D_s for the swelling

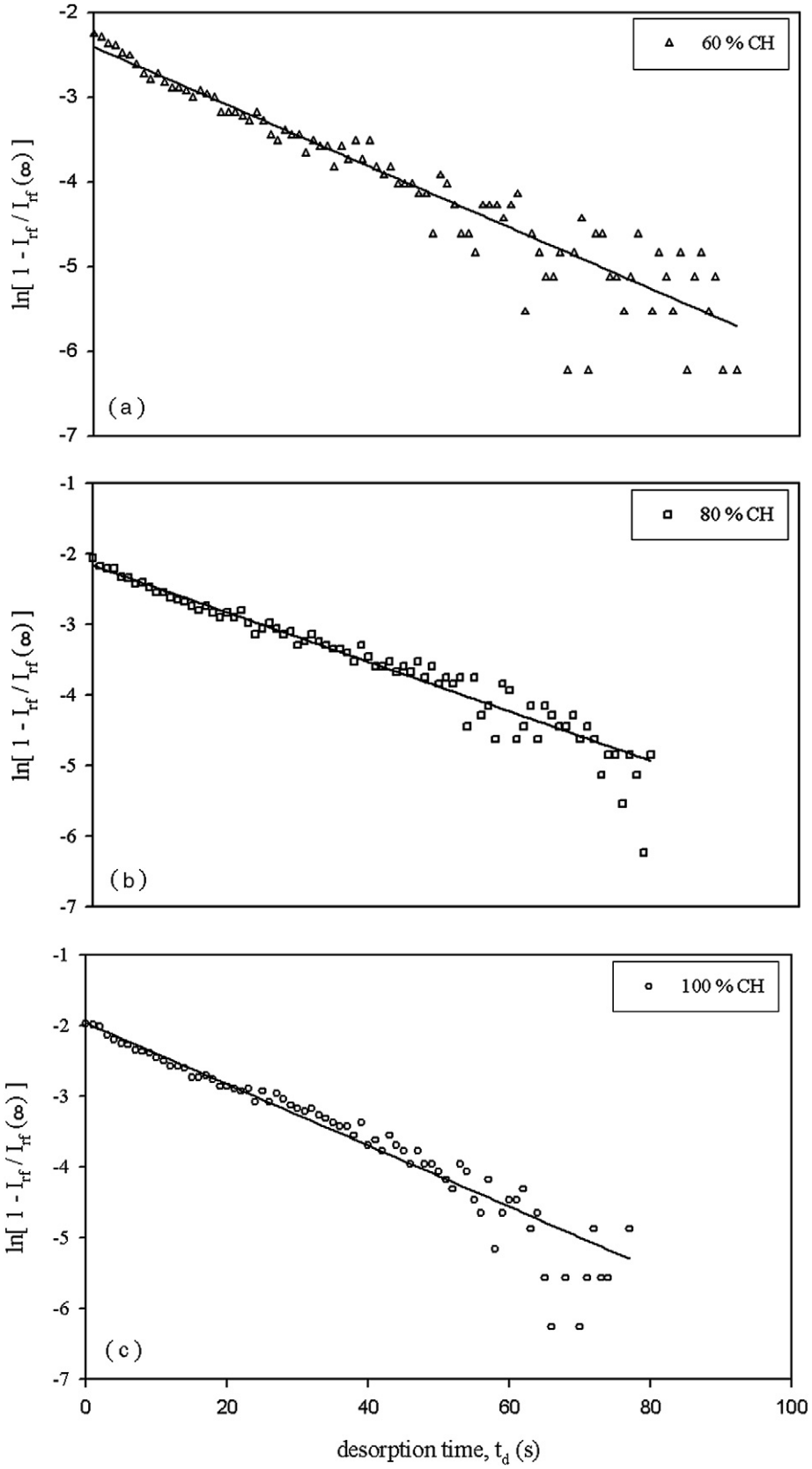

Fig. 6. Plot of the digitized data in Fig. 3b, which obey the relation given Eq. (9) where t_d is the desorption time and (a), (b) and (c) show the data for samples exposed to 60%, 80% and 100% saturated chloroform vapor content, respectively.

of polymeric film and those values are plotted in Fig. 5 versus saturated chloroform vapor content. It can be seen that diffusion coefficients, D_s is increased as the vapor content increased in the cell. In another words, a decrease in the vapor content prevents the film from swelling and the diffusion of chloroform molecules into polymeric film slows down.

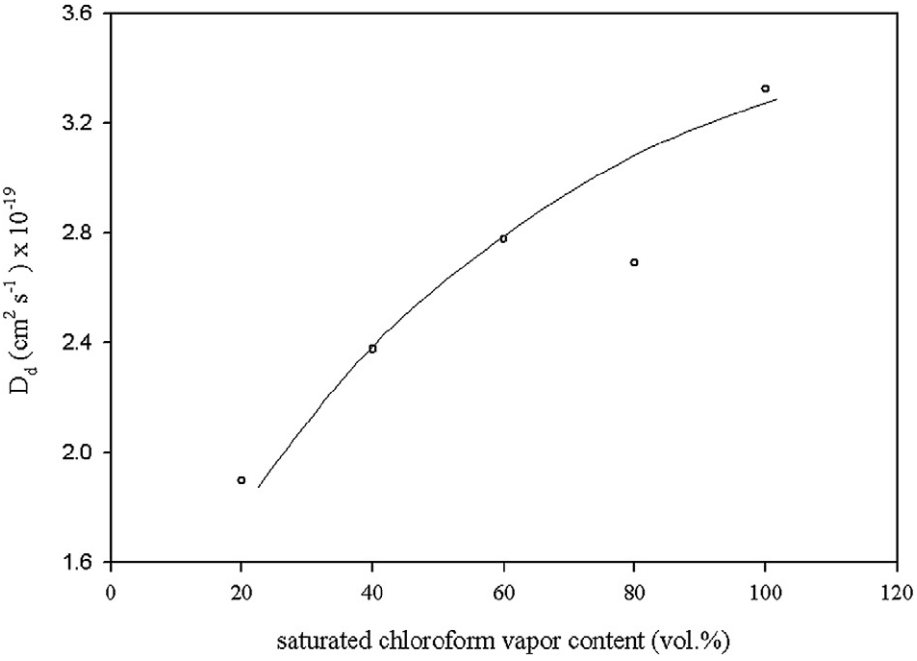

Fig. 7. The plot of desorption diffusion coefficients, D_d, versus the saturated chloroform vapor content.

Fig. 3b shows that reflected light intensity, I_{rf} from the swollen film is increased, as the desorption time, t_d is increased. Since reflected light intensity, I_{rf} is proportional to the amount of the organic vapor released from the polymeric film, the behavior of intensity curves in Fig. 3b may suggest that the longer the desorption time, the more chloroform vapor molecules have been released to surrounding area. The relationship between the fraction, M_t/M_∞ of the released saturated chloroform vapor from swollen polymeric film and reflected light intensity, I_{rf} can simply be expressed as:

$$\frac{M_t}{M_\infty} \approx \frac{I_{rf}}{I_{rf}(\infty)}. \tag{8}$$

Combining Eq. (8) with the logarithmic form of Eq. (5), the following equation can be obtained as:

$$\ln\left[1 - \frac{I_{rf}}{I_{rf}(\infty)}\right] = \ln\left[\frac{8}{\pi^2}\right] - \frac{D\pi^2}{a_0^2}t. \tag{9}$$

Desorption diffusion coefficients, D_d for saturated chloroform vapor can therefore be obtained using Eq. (9). The $I_{rf}/I_{rf}(\infty)$ data in Fig. 3b are fitted to Eq. (9) in which the slope of the linear curves produces the value of D_d. It can be seen that good linear fitting can be obtained in Fig. 6, which states that desorption model employed here is reliable for the polymeric film system. The plot of desorption diffusion coefficients, D_d versus the saturated chloroform vapor content is shown in Fig. 7. As expected, the release of vapor molecules from swollen polymeric film slows down as the vapor molecule content is decreased.

4. Summary

In conclusion, we introduced a model to employ the sorption behavior of An-PMMA polymeric film under exposure to different saturated chloroform vapor content in dry air. It is understood that the penetration of organic vapor molecules into the polymeric film is fast and the interdiffusion of polymer chains increases as the organic vapor content in air increases. This behavior can be interpreted in terms of the solubility parameter, δ of swelling agent and polymeric film. A decrease of saturated chloroform vapor content in the cell prevents the polymeric film from swelling since organic solvent chloroform and PMMA both have the same solubility parameter ($\delta = 19$ MPa$^{1/2}$). In another words, by increasing organic vapor content in the cell, swelling agent becomes a good solvent for the PMMA film. Diffusion coefficients, D_d for desorption is also strongly correlated with organic vapor content. As the polymeric film swells faster, the release of organic vapor from swollen film is faster during the desorption process. As a result, polymer-solvent interaction plays a dominant role during swelling and desorption processes.

References

[1] K. Manoli, D. Goustouridis, S. Chatzandroulis, I. Raptis, E.S. Valamontes, M. Sanopoulou, Polymer 47 (2006) 6117.
[2] B.K. Lavine, N. Kaval, D.J. Westover, L. Oxenford, Anal. Lett. 39 (2006) 1773.
[3] M.E.H. Amrani, P.A. Payne, R.M. Dowdeswell, A.D. Hoffman, Sens. Actuators B 57 (1999) 75.
[4] K.C. Persaud, S.M. Khaffaf, P.J. Hobbs, R.W. Sneath, Chem. Senses 21 (1996) 495.
[5] D.R. Baughman, Y.A. Liu, Ind. Eng. Chem. Res. 33 (1994) 2668.
[6] K.M. Mangold, K. Jüttner, Synth. Met. 101 (1999) 71.
[7] Y. Hirai, Kobunshi Ronbunshu 55 (1998) 2, 66.
[8] R. Ince, R. Narayanaswamy, Anal. Chim. Acta 569 (2006) 1.
[9] X. Yin, L. Hesselink, Appl. Phys. Lett. 89 (2006) 261108.
[10] J.M. Brockman, B.P. Nelson, R.M. Corn, Annu. Rev. Phys. Chem. 51 (2000) 41.
[11] S. Toyama, K. Aoki, S. Kato, Sens. Actuators B 108 (2005) 903.
[12] B.K. Lavine, D.J. Westover, N. Kaval, N. Mirjankar, L. Oxenford, G.K. Mwangi, Talanta 72 (2007) 1042.
[13] J. Crank, The Mathematics of Diffusion, Oxford Univ. Press, London, 1970.
[14] M. Erdogan, G. Hizal, U. Tunca, D. Hayrabetyan, O. Pekcan, Polymer 43 (2002) 1925.
[15] H. Arwin, D.E. Aspnes, Thin Solid Films 138 (1986) 195.
[16] E. Kretschmann, H. Raether, Z. Naturforsch. 23A (1968) 2135.
[17] A.V. Nabok, A.K. Hassan, A.K. Ray, O. Omar, V.I. Kalchenko, Sens. Actuators B 45 (1997) 115.
[18] C.B. Walsh, E.I. Franses, Thin Solid Films 347 (1999) 167.
[19] C.B. Walsh, E.I. Franses, Thin Solid Films 429 (2003) 71.
[20] O. Pekcan, N. Adiyaman, S. Ugur, J. Appl. Polym. Sci. 84 (2002) 632.